



## EXPERIMENTAL ANALYSIS OF STIFFENED PERFORATED COLD-FORMED STEEL MEMBERS UNDER COMPRESSION

Fattouh M. F. Shaker<sup>1</sup>, Mohamed M. Yehia<sup>2</sup>, Zekriat Mamdooh<sup>3</sup>.

<sup>1</sup> Associate Professor, Civil Eng. Department, Faculty of Eng. Mataria, Helwan University, Cairo, Egypt.

<sup>2</sup> Assistant Professor, Faculty of Eng. Mataria, Helwan University, Cairo, Egypt.

<sup>3</sup> Demonstrator, Faculty of Eng. Mataria, Helwan University, Cairo, Egypt.

E-mail: Zekriat.mamdooh@gmail.com

### ملخص البحث:

أصبح استخدام مقاطع الصلب المدعمة والمتقبة المشكّلة على البارد أكثر انتشاراً خصوصاً في استخدام قوائم المنشآت المعدنية، من أبرز تلك المنشآت هو نظام الأرفف المستخمة للتخزين و تستخدم تلك المقاطع في صناعة القوائم الخاصة به. هذا البحث يستعرض التحقيق المعملّي لدراسة سلوك تلك القوائم المصنوعة من مقاطع الصلب المدعمة والمتقبة المشكّلة على البارد و المعرضة لحمل الضغط المحوري. تم اختبار عينتين من العينات المتقبة تحت حمل الضغط المحوري، تشمل العينتين قطاعين مختلفين تبعاً لطول عصب القطاع المستخدم (90 و 110 مم) مع ثبات الارتفاع و السمك المساويان 1500 مم و 1.5 مم على التوالي. يتم أداء تلك الإختبارات المعملية للحصول على أقصى قوة تحمل، قياس مقدار الإزاحات الناتجة عن التحميل. و أيضاً تم توصيف السلوك الإنشائي الخاص بالعينات. إذن النتائج التي تم الحصول عليها من التجارب المعملية توضح الآتي: قيمة مقاومة الضغط النسبية القصوى أقل من واحد لكل العينات، مما يشير إلى أن العينات انهارت بسبب الإنبعاج، و يعد نوع الإنهيار الأساسي هو التفاعل بين الإنبعاج الكلي للعيّنة مع تشوه حافة القطاع. بالإضافة إلى أن تأثير طول عصب القطاع عند زيادته من 90 مم إلى 110 مم على قيمة مقاومة الضغط المحورية القصوى يعتبر تأثير هامشي لا يذكر.

الكلمات المفتاحية: الصلب المشكّل على البارد، المدعمة، المتقبة، إختبار الضغط المحوري و التفاعل بين الإنبعاج الكلي مع تشوه حافة القطاع.

### ABSTRACT:

The use of stiffened perforated cold-formed steel (CFS) sections are becoming increasingly popular for upright members in col-formed steel structures, the main application is steel storage perforated rack uprights. This paper presents an experimental investigation into the behavior of stiffened perforated cold-formed steel (CFS) uprights subjected to axial compression. A total of two perforated specimens were tested under axial compression, including two different cross-sections according to the overall web length were used (90 and 110 mm) with constant total height and thickness are 1500 mm and 1.5 mm respectively. These tests were performed to obtain the ultimate load applied, along with the measurement of the displacements. Also, their structural behavior was described. Therefore, the results obtained from test showed that the value of the normalized ultimate compression strength smaller than unity for specimens, indicating that the specimens failed by buckling, the main failure mode is distortional-global buckling interaction. In addition, the web length has a

marginal effect on ultimate axial compression capacity when the web increased from 90 mm to 110 mm.

**Key words:** Cold-formed steel, Stiffened, Perforation, Axial compression test and Distortional-global buckling interaction.

## 1. Introduction.

Cold-formed profiles are widely used in component elements of factories and racking systems (purlins, side girt, beams and up-rights). Stiffened perforated cold-formed steel (CFS) sections are the most popular cross-sections using in racking systems especially the uprights. The main functions of stiffeners are to subdivide the slenderest wall into several plates to make the cross section fully effective and enhancement its efficiency. The main functions of perforations to allow the other members to connected to the uprights such as: pallet rack beams and bracing for assemblage the industrial storage systems, parts of the racking system shown in Figure 1. with the growing use of industrial storage systems in recent years, it is necessary that the structural behavior of the uprights be studied.

In this paper, an experimental investigation into the behavior of stiffened perforated col-formed steel uprights subjected to axial compression is presented. Compression test were conduct on two specimens with constant specimens height and thickness but include two cross-sections have different web length. Based on the test investigations, the influence of web length on the ultimate axial compression capacity and the behavior and failure mode of uprights are studied and observed.

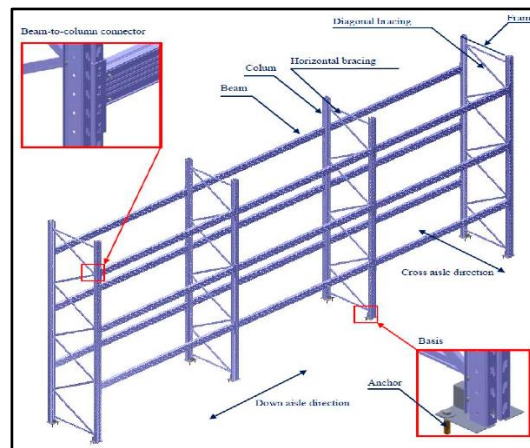


Figure 25. Parts of the racking system.

## 2. Experimental Program.

### 2.1. Specimens.

C channel section was used for two stiffened perforated specimens have height (H)=1500 mm with thickness (t)=1.5 mm, 2 web lengths (L<sub>w</sub>) used 90 and 110 mm with constant flange length (L<sub>f</sub>)=80 mm. Table 1 show the properties of test specimens, (P) means perforated specimen. Figure 2 shows the cross-sectional geometry and illustrates the typical perforation locations and dimensions at the web and the flange.

Table 1: Properties of Test Specimens.

Specimen	L <sub>w</sub> (mm)	L <sub>f</sub> (mm)	t (mm)	H (mm).	A <sub>gross</sub> (mm <sup>2</sup> )	A <sub>net</sub> (mm <sup>2</sup> )
C90-1.5-P-1500	90	80	1.5	1500	455.35	407.65
C110-1.5-P-1500	110	80	1.5	1500	510.91	463.21

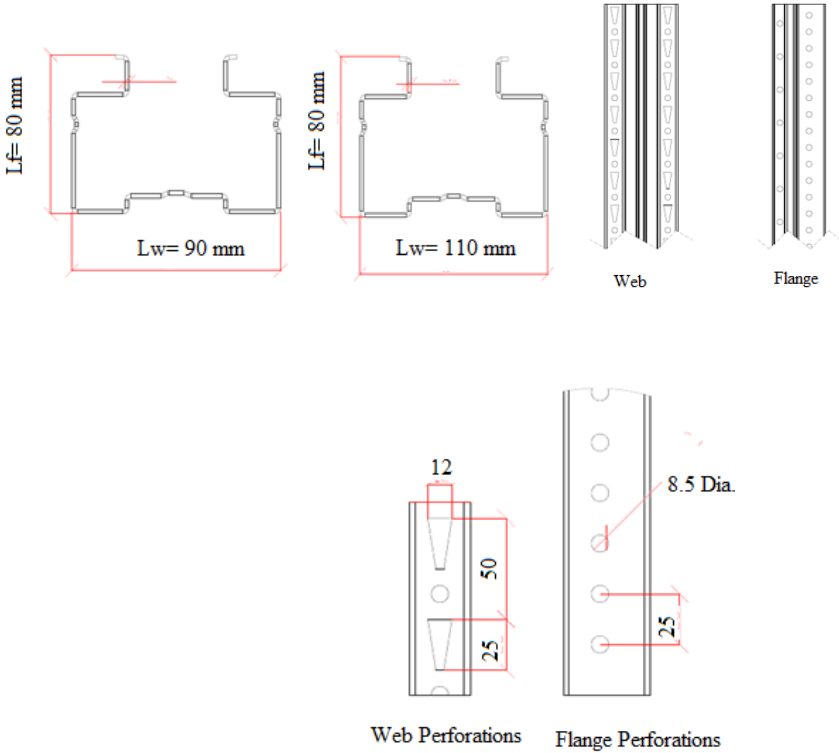


Figure 2. Cross-sectional geometries, perforation positions and regular perforations in web and flanges.

## 2.2. Material Properties.

The mechanical characteristic of the steel used has yield strength  $383 \text{ N/mm}^2$ .

## 2.3. Test Setup and Instrumentations.

The experimental tests were performed using hydraulic jack with a capacity 1000 kN of compression to apply an axial load. In the tests, the specimens were placed vertically. The boundary conditions of specimens hinged from top and bottom. All specimens under axial compression and connected with several dial gauges of 0.1 mm accuracy connected to LVDT system were positioned at the middle height to determine the displacements of the flange, the web and the axial shortening displacement then demonstrate the deformations of members load-displacement curves. The experimental arrangement of upright test is shown in Figure 3. The axial load was applied from the upper incrementally, the test stopped when the load applied on the specimen reached the failure point. Deflection recorder by the LVDT via the dial gauge readings were recorded at every load increment.

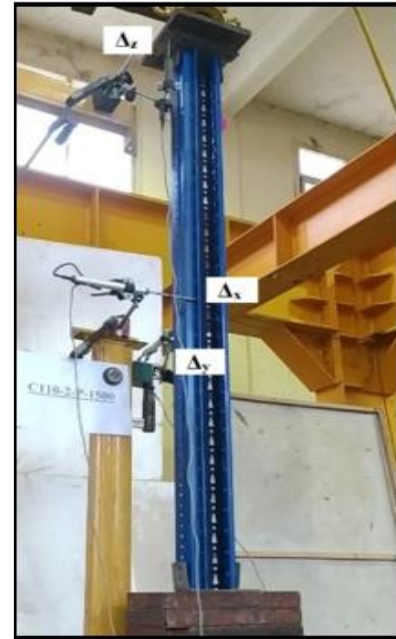


Figure 3. Experimental arrangement.

## 3. Test Results.

### 3.1. Specimen C90-1.5-P-1500.

In Figure 4 the buckling mode of this specimen is dominated by the distortional-flexural buckling interaction (DB+FB). Figure 5 shows a total large lateral displacement of web ( $\Delta y$ ) and the equivalent lateral displacement of flanges ( $\Delta x$ ) that indicate not only flexural buckling exists, but also that distortional buckling has an influence on the failure mode of the specimen. The compression ultimate capacity of this specimen obtained from test is 90.1 kN for axial shortening displacement ( $\Delta z$ ) equal 6 mm as shown in Figure 6.



Figure 4. Buckling failure mode of C90-1.5-P-1500 specimen.

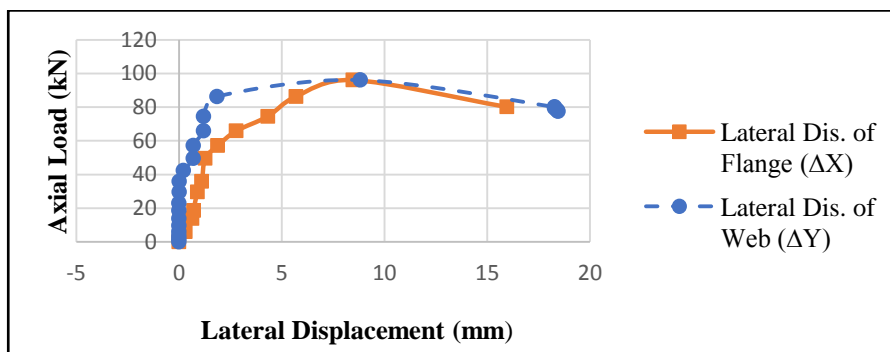


Figure 5. Load –lateral displacement curves for C90-1.5-P-1500 specimen.

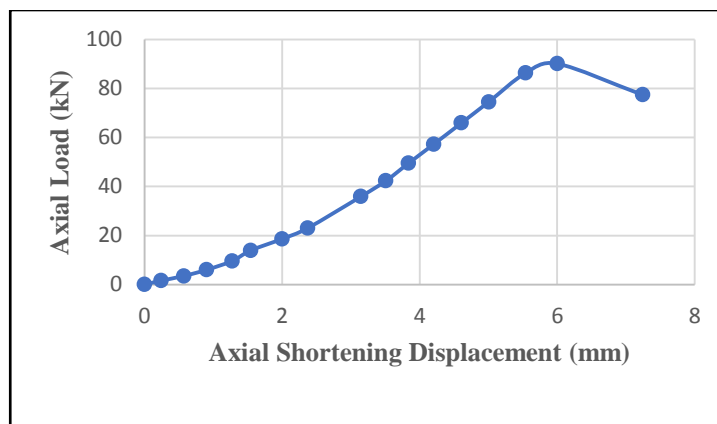


Figure 6. Load –axial shortening displacement curve for C90-1.5-P-1500 specimen.

### 3.2. Specimen C110-1.5-P-1500.

The buckling mode of this specimen is dominated by the distortional-flexural buckling interaction (DB+FB). However, the distortional buckling mode is not shown clearly as shown in Figure 7. Figure 8 shows the relation between the applied axial load versus the total lateral displacement of web ( $\Delta y$ ) and lateral displacement of flanges ( $\Delta x$ ). From the curve can be observed that not only flexural buckling exists, but also that distortional buckling has an influence on the failure mode of the specimen. The compression ultimate capacity of this specimen obtained from test is 100.4 kN for axial shortening displacement ( $\Delta z$ ) equal 2.5 mm as shown in Figure 9.



Figure 7. Buckling failure mode of C110-1.5-P-1500 specimen.

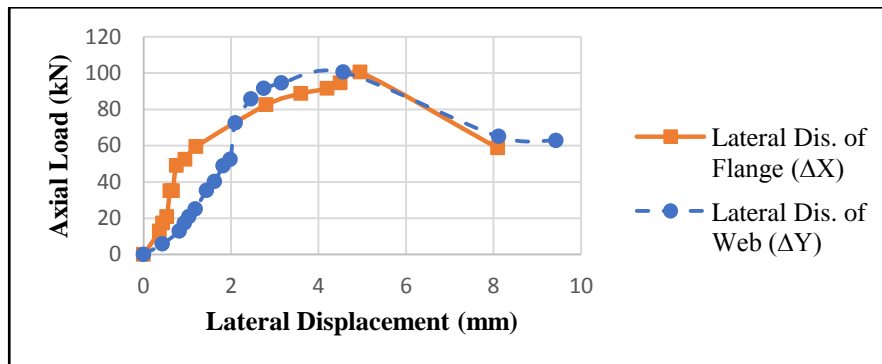


Figure 8. Load-lateral displacement curves for C110-1.5-P-1500 specimen.

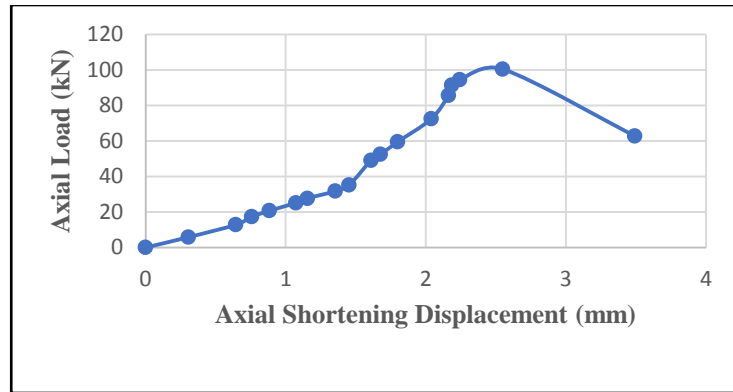


Figure 9. Load –axial shortening displacement curve for C110-1.5-P-1500 specimen.

#### 4. Analysis of Test Results.

The shown Table 2 presents compression ultimate capacity for specimens, the failure mode and the normalized ultimate compression strength “the ultimate strength obtained from the test was divided by yield load of the gross cross section ( $P_y = A_g \times F_y$ )”

The value of normalized ultimate compression strength “the ultimate test strength: yield load ratio” ( $P_{u,test}/P_y$ ) is approximately 0.5. The value was smaller than unity for specimens, indicating that the specimens failed by buckling and the full cross-sectional capacity could not be developed.

Table 2: Ultimate loads, normalized ultimate compression strength and failure modes.

Specimen	$P_{u,test}$ (kN)	$P_{u,test}/P_y$	Failure mode
<b>C90-1.5-P-1500</b>	90.1	0.52	(DB+FB)
<b>C110-1.5-P-1500</b>	100.4	0.51	(DB+FB)

To study the effect of overall web length variations, there are two different cross section types with two different overall web length (90 and 110 mm) all sections had constant thickness and height equal 1.5 mm, 1500 mm respectively.

The load-axial shortening displacement curves for the specimens with perforations are plotted in Figure 10. A comparison of perforated specimens with different web lengths shows that the specimens with the larger web lengths have a higher axial compression strength because the larger web had larger cross-sectional area. However, when overall web length of section increases from 90 mm to 110 mm the percentage increase in cross-section area more than the percentage increase in ultimate capacity as shown in Table 3. Therefore, uneconomical decision to increase the web length from 90 mm to 110 mm to obtain a higher

compressive strength. Figure 11 shows that the web length has a marginal effect when the web increased from 90 mm to 110 mm.

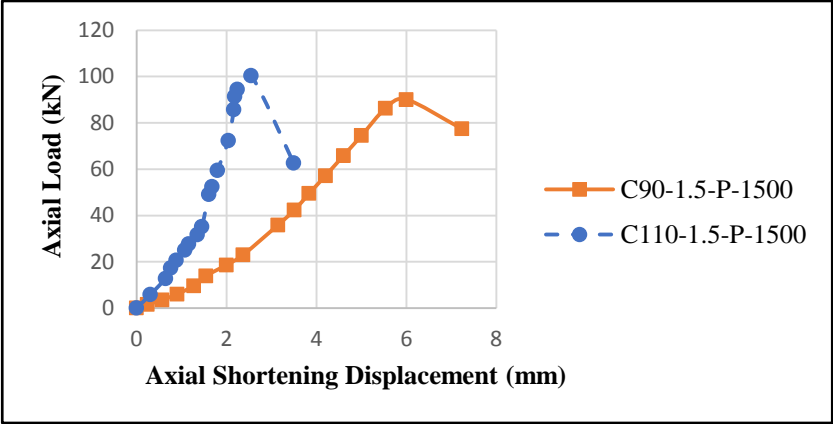


Figure 10. Comparison of the load-axial shortening displacement curves for perforated specimens with different web lengths.

Table 3: The percentage increase in ultimate capacity for perforated specimens with different web lengths.

Specimen height	Changing in cross section type	% Increase in cross-section area	% Increase in ultimate capacity
1500 mm	From C90-1.5-P to C110-1.5-P	13.6%	11.4%

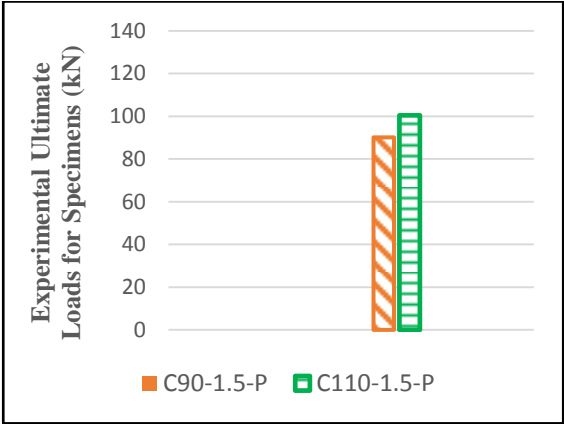


Figure 11. Effect of web lengths on axial compression strength.



## 5. Summary and Conclusions.

This paper has presented an experimental investigation into the behavior of stiffened perforated CFS sections subjected to axial compression. An experimental results were reported. The failure modes, axial capacity, load-axial shortening, load-lateral displacement relationships are discussed. The effect of the overall web length of cross-sections was investigated.

Based on the experimental and results presented in this paper, the following conclusions can be drawn:

- The normalized ultimate compression strength “the ultimate test strength: yield load ratio” ( $P_{u, \text{test}}/P_y$ ) is approximately 0.5. The value was smaller than unity for specimens, indicating that the specimens failed by buckling.
- The test results showed that for the specimens with total height 1500 mm, the interaction between distortion buckling and global buckling was the final failure mode.
- The web length has a marginal effect on ultimate axial compression capacity when the web increased from 90 mm to 110 mm.

## 6. References.

1. **Pu, Y., Godley, M. H. R., Beale, R. G., Lau, H. H.**, Prediction of ultimate capacity of perforated lipped channels, *Journal of Struct. Eng.* (1999) 125:510-514.
2. **Moen, D.C., Schafer, B. W.**, Experiments on cold-formed steel columns with holes, *Journal of Thin-Walled Struct.* 46 (2008) 1164-1182.
3. **Zhao, X., Ren, C., Qin, R.**, An experimental investigation into perforated and non-perforated steel storage rack uprights, *Journal of Thin-Walled Struct.* 112 (2017) 159-172.
4. **Xiang, Y, Zhao, X., Shi, Y., Xu, L., Xu, Y.**, Experimental investigation and finite element analysis of cold-formed channel columns with complex edge stiffener, *Journal of Thin-Walled Struct.* 152 (2020) 106769.
5. **Vujanac, R., Miloradovid, N., Vulovic, S., Pavlovic, A.**, A comprehensive study into the boltless connections of racking systems, *Journal of Metals* (2020). 10(2). 276.